IOSR Journal of Applied Physics (IOSR-JAP)
e-ISSN: 2278-4861.Volume 8, Issue 5 Ver. III (Sep - Oct. 2016), PP 01-08
www.iosrjournals.org

Calculations of Photo field emission current in zirconium carbide (ZrC) by using Green's functions method

LeishangthemNirmala Devi[1], Ram Kumar Thapa[1], Lalrinpuii[2] and Gunakar Das[2*]

[1]*Department of Physics, Condensed Matter Theory Research Group, Mizoram University, Aizawl 796 004, Mizoram*

[2]*Department of Physics, Government Kolasib College, Kolasib 796081,Mizoram.*

Abstract: *In this report, we will present results of Photofield emission current (PFEC) from zirconium carbide (ZrC) by using Green's function in which the basic functions are deduced by using Projection Operator method of Group Theory.The vector potential of interest are the ones developed by Bagchi and Kar . Results of PFEC in ZrC are compared with the density of state (DOS) calculated by using the density functional theory which is implemented in wien2k code.*

Keywords: *Band structure, Density functional theory, Photofield emission ; Projection operator; Vector potential.*

I. Introduction

Photo field emission (PFE) is a combined process due to photoemission and cold emission by the application of high electric field. The electrons are usually below the Fermi level hence a strong electric field will emit the electron outside into the vacuum which produces photo field emission current (PFEC).There have been several groups of experimental and theoretical study on PFE [5-11].They have included the effect of surface photo excitation mechanism. For example Caroli *et al* [12] emphasized the non-equilibrium aspects of PFE and presented the phenomena in terms of second-order perturbation theory. Taranko [13], Bagchi [14], Schwartz and Cole [15] calculated photofield energy distribution assuming different surface potential barriers. A general characteristic of these theories is the triangular-shaped energy distribution. Lee [5],Gao and Reifenberger [7] and Schwartz and Schaich [8]have considered also the effect of image potential barrier on the work function of metal in their calculation of PFE. The transmission probability function calculated by them was acceptable. In mostof the theoretical study of PFE, a free electron model has been used to define the bulk and surface potential. But in these cases, the initial state wavefunction was not suitably defined.

In this report, we have calculated photofield emission current (PFEC) by using Green's function method for zirconium carbide (ZrC).PFEC is calculated by using the formula given by Gao and Reifenberger [7]. For the calculation of PFEC, the initial state wavefunction as deduced by Thapa and Das [1] by using the projection operator method of group theory will be used. Dielectric model deduced by Bagchi and Kar [2] is used for obtaining the vector potential in the surface region. In all these, the values used for real and imaginary dielectric constants are deduced by using wien2k code [4]. In this code, full-potential linearised augmented plane wave (FP-LAPW) method is used based on density functional theory [4].

II. Theoretical Formalisms

We have considered a *p*-polarised radiation of photon energy $\hbar\omega$ incident on the metal surface. The surface normal is defined by z-axis which is perpendicular to the xy-plane. This incident radiation, usually a laserbeam, causes the transition of electrons from the initial state $|i\rangle$ to final state $|f\rangle$. We consider initial states to be electron states lying below the Fermi level, and final states are states in the vacuum (detector). Therefore, the matrix element for this transition can be given as

$$M_{fi} = \langle f | \boldsymbol{A}.\boldsymbol{p} + \boldsymbol{p}.\boldsymbol{A} | i \rangle \tag{1}$$

where $\boldsymbol{p} = -i\hbar\nabla$ is momentum operator and $\boldsymbol{A}$ is the vector potential, the commutator $\boldsymbol{A}.\boldsymbol{p}$ with the Hamiltonian $\boldsymbol{H}$ is given by

$$[\boldsymbol{A}.\boldsymbol{p}, \boldsymbol{H}] = -i\hbar\, \boldsymbol{A}.\nabla V + \frac{\hbar^2}{2m}\nabla^2(\boldsymbol{A}.\boldsymbol{p}) + \frac{i\hbar}{m}\nabla(\boldsymbol{A}.\boldsymbol{p}).\boldsymbol{p} \tag{2}$$

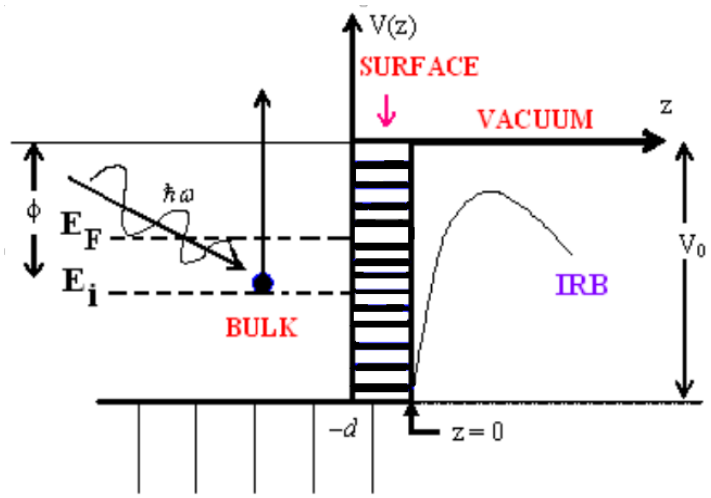

Fig. 1. Model potential used for photofield emission calculation. Here E_F is the Fermi level, E_i is the initial state energy of the electron, IRB is the image rounded barrier potential, V_o is the potential barrier.

From Eq. (1) and Eq. (2), we have

$$M_{fi} = \frac{2i}{\omega}\langle f \,|\, \boldsymbol{A}.\nabla V \,|\, i\rangle + \frac{\hbar}{m\omega}\langle f \,|\, \nabla^2 \boldsymbol{A}.\boldsymbol{p} \,|\, i\rangle - \frac{2i}{m\omega}\langle f \,|\, \nabla.(\boldsymbol{A}.\boldsymbol{p}).\boldsymbol{p} \,|\, i\rangle - i\hbar\langle f \,|\, \nabla.\boldsymbol{A} \,|\, i\rangle \tag{3}$$

The vector potential for the bulk ($z < -d$), surface ($-d \le z \le 0$) and vacuum $z > 0$ regions is given by

$$\tilde{A}_{\omega}(z) = \begin{cases} -A_o, & z < -d \\ -A_o \dfrac{d\varepsilon(\omega)}{[1-\varepsilon(\omega)]\, z + d}, & -d \le z \le 0 \\ -A_0 \,.\, \varepsilon(\omega), & z > 0 \end{cases} \tag{4}$$

where, $$A_o = -\frac{\sin 2\theta_i}{[\varepsilon(\omega) - \sin^2\theta_i]^{\frac{1}{2}} + \varepsilon(\omega)\cos\theta_i}$$

The matrix element M_{fi} of Eq. (3) can be expanded in one-dimension along *z*-axis as

$$M_{fi} = \int_{-d}^{0} \psi_f^* A_z \frac{dV}{dz}\psi_i dz + \int_{-d}^{0} \psi_f^* \frac{d^2 A_z}{dz^2}\left(-i\hbar\frac{d}{dz}\right)\psi_i dz + \int_{-d}^{0} \psi_f^* \frac{dA_z}{dz}\left(-\hbar^2\frac{d^2}{dz^2}\right)\psi_i dz + \int_{-d}^{0} \psi_f^* \frac{dA_z}{dz}\psi_i dz. \tag{5}$$

Now the photoexcited electrons are in final state with energy $E_f = E_i + \hbar\omega$ due to absorption of photon energy. These photoexcited electrons lie below the vacuum level. When a strong electric field will be applied experimentally, the photoexcited electrons are emitted to vacuum region by passing through surface potential barrier. The high static electric field decreases the work function of the metal causing thereby the Schottky effect which brings the image potential effect. This will reduce the height of the step potential and the work function at the surface as shown in Fig. 1.The photofield emission current density formula is given by [7].

$$\frac{dj}{dE} = -\frac{e^3}{2\hbar^4\omega^3}\frac{n}{\Omega}(\hat{\varepsilon}.\hat{z})^2 \, f\left(E - \hbar\omega\right) \int_{-V_O+\hbar\omega}^{E} dW \, \frac{D(W)\left|M_{fi}\right|^2}{\left[W\left(W - \hbar\omega\right)\right]^{\frac{1}{2}}} \tag{6}$$

where $\frac{n}{\Omega}(\hat{\varepsilon}.\hat{z})^2 = \left|\frac{A_\omega(z)}{A_0}\right|^2 = \left|\tilde{A}_\omega(z)\right|^2$, and $A_\omega^z(z)$ is the *z*-component of vector potential along *z*-axis, A_0 is the amplitude of vector potential associated with the incident radiation, $f(E-\hbar\omega)$ is the Fermi-Dirac distribution function, D (W) is the quantum mechanical transmission probability, the energy of the photoexcited electron is

$$E_{KIN} = W + \frac{\hbar^2 k_{\parallel}^2}{2m}$$

where W is the normal component of kinetic energy E_{KIN}. These electrons will travel across the surface potential barrier which is deformed by the applied electrostatic field and the image potential barrier. The transmission probability $D(w)$ in this model is given by [16]

$$D(W) = \frac{W^{\frac{1}{4}}\sqrt{\pi}}{(\hbar eF)^{\frac{1}{6}}}\left(\frac{2ik_i}{ik_i+\chi}\right)(2m)^{\frac{1}{12}}\exp\left[-i\left(\frac{2}{3}\frac{W^{\frac{3}{2}}\sqrt{2m}}{\hbar eF}+\frac{\pi}{4}\right)\right] \tag{7}$$

and $$V(z) = -V_0 - e\,F\,z - \frac{e^2}{4z} \tag{8}$$

Therefore $V(z)$ is called image rounded potential barrier (IRB) which is shown in Fig. 1.

III. Initial state wave functions

Initial (ψ_i) state wavefunction required in the matrix element in Eq.(6) are derived by using projection operator method as deduced by Thapa and Das [1] for photofield calculations.To calculate the initial state wavefunction ψ_i, we have assumed the crystal potential of the solid which is defined by δ - potential and represented by the Kronig-Penny potential. The potential is periodic with the periodicity of the lattice as shown in Fig 1. In one dimension, one can write ψ_i as

For one dimensional case, the Schrödinger equation can be written as

$$\left(\nabla^2 + k_i^2\right)\psi(z) = V(z)\psi(z), \tag{9}$$

where $k_i^2 = \frac{2m}{\hbar^2}E_i$. If Green function of a free particle is defined as $G(z,y)$, then the equation for a point source is,

$$\left(\nabla^2 + k_i^2\right)G(z,y) = \delta(z-y). \tag{10}$$

In terms of Green function, Schrodinger equation Eq. (9) can now be replaced by the integral equation

$$\psi(z) = \int_{-\infty}^{+\infty} V(y)\psi(y)G(z,y)\,dy. \tag{11}$$

Considering the periodicity of the crystal gives $V(v+na) = V(y)$, and the Bloch-Floquet theorem yields

$$\psi(y+na) = e^{ik_i na}\psi(y). \tag{12}$$

Eq. (11) can now be written as

$$\psi(z) = \sum_{n=-\infty}^{\infty} e^{ik_i na}\int_0^a V(y)\psi(y)\,G(z,y+na)\,dy. \tag{13}$$

Putting $s = z - y$ and $t = s - a\left[\frac{s}{a}\right]$, we get

$$\psi(z) = -\frac{1}{2k_i}\int_0^a e^{ika\left[\frac{s}{a}\right]}\frac{e^{ika}\sin k_i t - \sin k_i(t-a)}{\cos k_i a - \cos ka}\psi(y)V(y)\,dy\ . \tag{14}$$

The direct matching procedure for the solution of Schrödinger equation with Kronig-Penney model potential incorporated gives

$$\psi(z) = 2iC\,\frac{e^{ika}\sin k_i z - \sin k_i (z-a)}{e^{ika} - e^{-ik_i a}}. \tag{15}$$

When $z = 0$ $\qquad \psi(0) = 2iC\,\frac{\sin k_i a}{e^{ika} - e^{-ik_i a}}$. (16)

For $k = \frac{\pi}{a}$ (taking only positive value)

$$\psi(0) = -2iC\,\frac{\sin k_i a}{1 + cosk_i a - i\sin k_i a}. \tag{17}$$

The initial state wavefunction $\psi_i(z)$ in terms of Green's function (Eq. 15) is given by

$$\psi_i(z) = \begin{cases} \psi(z) + R\psi^*(z) & z \le 0 \ (bulk \,\&\, surface) \\ T\,e^{-\chi z} & z \ge 0 \ (vacuum) \end{cases} \tag{18}$$

where $\psi^*(z)$ is the complex conjugate of $\psi(z)$, R is the reflection coefficient, T is the transmission coefficient across the boundary plane and $\chi_0^2 = \frac{2m}{\hbar^2}(-V_0 - E_i)$ with V_0 as the potential at the surface which an electron encounters while transmitting through the boundary surface. Matching the wavefunction and its derivatives at $z = 0$ gives the value of coefficients R and T as

$$R = \frac{-\chi + \mu - ik}{\chi - \mu - ik} \tag{19}$$

and $\qquad T = \sigma\left(\frac{-2ik}{-\chi - \mu - ik}\right)$ (20)

where , $\sigma = \frac{p}{k_i a}\psi(0)\frac{\sin k_i a}{\cos ka - \cos k_i a}$ (21)

Also p is the strength of the δ - potential barrier and it is assumed to be positive and μ is used as converging factor

Now introducing the atomic orbital $\Phi(z)$, which includes the basis function derived by projection operator method of group theory[1], the final form of initial state wavefunction can be represented by

$$\psi_i(z) = \begin{cases} \sigma\left[\Phi(z)e^{ikz} + R\Phi^*(z)e^{-ikz}\right], & bulk \,\&\, surface\, d \le 0 \\ T\,e^{-\chi z}, & vacuum\, d \ge 0 \end{cases}. \tag{22}$$

Putting $\psi(0) = -2iC\,\frac{\sin k_i a}{1 + cosk_i a - i\sin k_i a}$ in Eq. (21), we finally get

$$\sigma = iC\,\frac{\chi^2 b}{k_i}\left(\frac{\sin k_i a}{1 + \cos k_i a - i\sin k_i a}\right)\left(\frac{\sin k_i a}{1 + \cos k_i a}\right) \tag{23}$$

The description of the final state wavefunction $|\psi_f\rangle$ used is given by [16] as

$$\psi_f(z)=\begin{cases}\left(\dfrac{m}{2\pi\hbar^2 q_f}\right)^{\frac{1}{2}}\dfrac{2q_f}{q_f+k_f}e^{-\alpha|z|}e^{ik_f z}.e^{i\vec{k}_{\parallel}.\vec{r}_{\parallel}}, & d<0 \quad (bulk\ \&\ surface)\\ \left(\dfrac{m}{2\pi\hbar^2 q_f}\right)^{\frac{1}{2}}\left[e^{iqz}+\dfrac{q_f-k_f}{q_f+k_f}e^{-iq_f z}\right].e^{i\vec{k}_{\parallel}.\vec{r}_{\parallel}}, & d>0 \quad (vacuum)\end{cases} \tag{24}$$

Where, $k_f^2=\dfrac{2mE_f}{\hbar^2}-\vec{k}_{\parallel}^{\,2}$; $q_f^2=\dfrac{2m}{\hbar^2}\left(E_f+V_0\right)-\vec{k}_{\parallel}^{\,2}$ *and* $E_f=E_i+\hbar\omega$

In Eq. (24), the scattering factor $e^{-\alpha|z|}$ is present on the surface and bulk sides to take into account the inelastic scattering of the electrons. The wavefunctions given by Eqs. (22) and (24) are then used in Eq. (6) to calculate photofield emission current by writing FORTRAN program.

IV. Results and Discussion

4.1 Calculation of photo field emission current

We present here the behavior of photo field emission current (PFEC) for zirconium carbide (ZrC), which is calculated by using the projection operator [1] which is incorporated into the Green's function. PFEC is calculated as a function of initial state energy (E_i), the applied high static field (F) at surface and bulk region. The required parameters used for calculations of model are: surface width (d) = 4.7126 A^0, initial state energy (E_i) = 2.397 eV, potential barrier height at the surface (V_0) = 13.5803 eV, work function (ϕ) = 3.5 eV, Fermi energy (E_F) = 10.08 eV, and scattering factor (α) = 0.35.

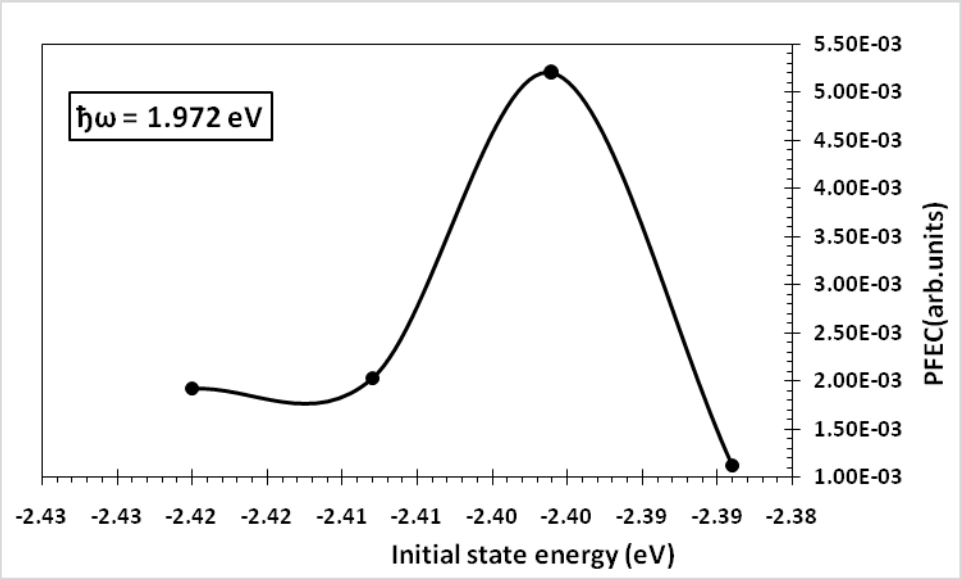

Fig. 2. Plot of Photo field emission current against initial state energy for photon energy =1.972*eV*
Here Fermi level E_F= 0.0 is taken as reference level, and the angle $\theta_i = 45^0$.

In Fig. 2, we have shown the results of the calculated PFEC as a function of initial state energy (E_i) for photon energies $\hbar\omega$ =1.972*eV*. Here the value of applied electric field (F) is equal to 4 X 10^9 V/m. and initial state energy E_i is taken below the Fermi level (E_F = 0.0). We have found that PFEC a maximum peak occurs at E_i = 2.396 eV below the Fermi level.

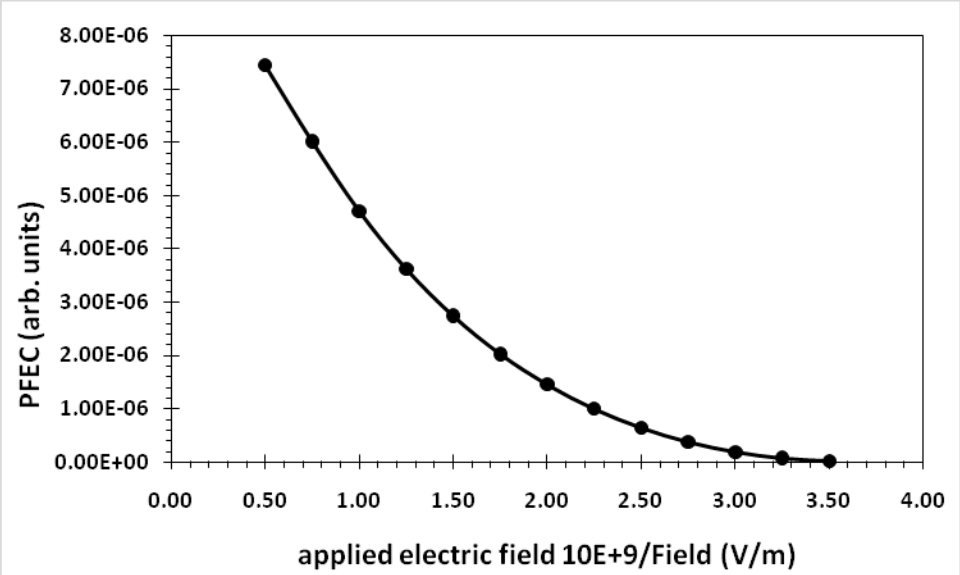

Fig. 3. Plot of photofield emission current against applied electric field for photon energy = 1.972 *eV*. The angle of incident photon radiation is $\theta_i = 45^0$.

In Fig. 3, we have shown the results of calculated PFEC as a function of the applied electric field (*F*) for photonenergy $\hbar\omega$ = 1.972 eV. We have chosen the initial state energy E_i = 1 eV below Fermi level (E_F = 0.0). From the plot, we find that as the value of applied electric field (*F*) increases, photofield emission current (PFEC) decreases from a high value towards minimum in an exponential manner. The exponential decrease in photofield emission current is due to presence of exponential term in calculation of transition probability *D(W)* formula given by Eq. (7).

4.2 Dos and Band structures

In this section, we have presented the calculated total and partial density of states (DOS) and the energy band structures for ZrC by using the Generalised Gradient Approximation (GGA) within the density functional theory [3] which is implemented in wien2k code [4]. In Fig. 8, we have shown the total density of states of ZrC, Zr and C respectively. From this plot, we find that maxima in total DOS of ZrC occurs at 2.402 eV below the Fermi level (E_F=0). We also find that the maxima inDOSpeak forZr and C occurs at 2.402 eV and 2.41 eV respectively below the Fermi level which is coinciding with the occurrence in peak for total DOS for ZrC. In the conduction region, the first peak in the total DOS of ZrC occurs at 5.453 eV above the Fermi level. Similarly the first peak in total DOS of Zr and C also occur at 5.453 eV and 5.44 eV respectively above the Fermi level. The second peak in total DOS of ZrC, occurs at 7.859 eV. The second peak in total DOS of Zr is occurred at 7.859 eV but in case of C atom the contribution in conduction region is negligible. The third peak in total DOS for ZrC, Z and C are very small in height and hence are neglected.

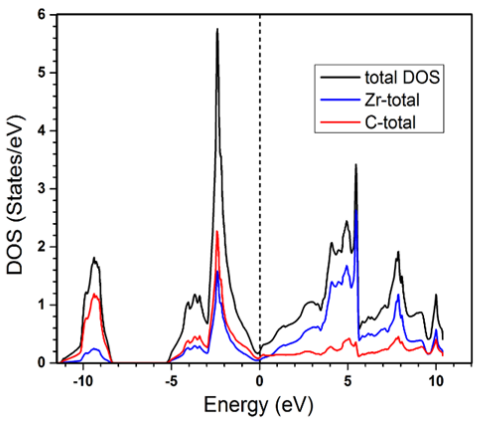

Fig. 4. Plot of total DOS for ZrC, Zr and C Fermi level is located at 0.

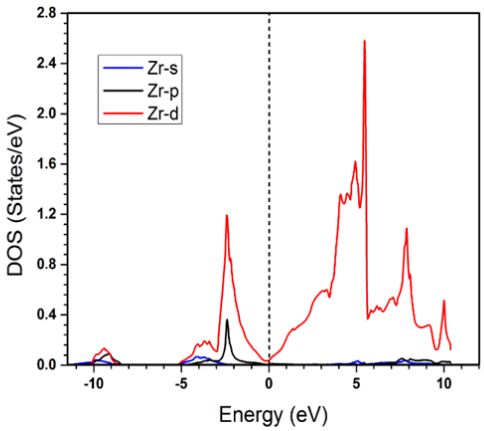

Fig.5. Plot of partial DOS of Zr. Fermi level is located at 0.

.

In Fig. 5, we have plotted the partial DOS plots of Zr atom. We find from this plot that the peak in partial DOS of Zr occurs at 2.402 eV below the Fermi level in the valence band which is contributed by *p* and *d*-state electrons of Zr atom. However the contribution of *p*-state electrons is very less compared to contribution by *d*-state electrons. The contribution of *s*-state electrons is very small and hence neglected. In the conduction band, the first maxima take place at 5.465 eV above the Fermi level. This peak is also contributed by the *d*-state electrons. The Second and third peaks in the partial DOS plot of Zr atom occur at 7.865 eV and 10.0 eV above the Fermi level respectively which is also contribution by the *d*-state electrons. In conduction band, contribution of *s* and *p*-state electrons of Zr atom is negligible which is evident from the low peak of DOS plot shown in Fig. 5.

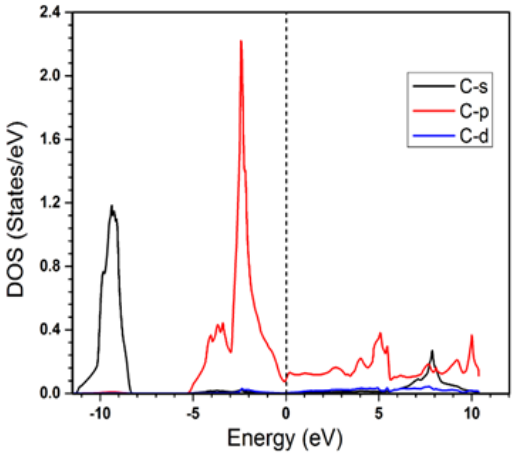

Fig.6. Plot of Partial DOS for C.

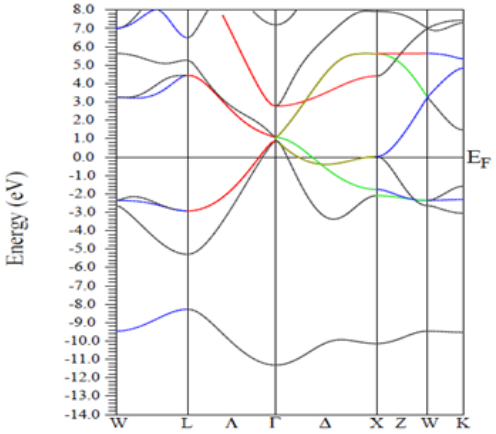

Fig. 7. Plot of Band structures for ZrC.

In Fig. 6, we have plotted the partial DOS of C atom. From this plot we have found that the peak in DOS occurs at 2.41 eV below the Fermi level in the valence band which is contributed by *p*-state electrons of C atom. The contributions of s and d-state electrons of C atom are negligible in the valence band. In the conduction band, very less amount of contribution is coming from the *s* and *p* state electrons. In case of conduction band we have found two small peaks in partial DOS plot of C atom occur at 5.065 eV and 7.865 eV above the Fermi level respectively. These peaks are contributed by the *p*ands-state electrons of C atom respectively. The small peak occurs at 10.0 eV is contributed by *p*-state electros of C atom. Contribution to partial DOS of C atom by *d*- state electrons is negligible which is evident from the partial DOS plot of C atom shown in Fig. 7. Hence the main Contribution to partial DOS of C atom in both valence and conduction band is *p*-state electrons.

We have also calculated the energy band structures of ZrC which are shown in Fig. 7.The band structure of ZrC has face centred cubic (fcc) and five high symmetry points indicated by W, L Γ, X and K with origin as Γ. The DOS plots shown in Figs. 1,2 and 3 supplements the band structures of the system. The lowest lying bands are due to *s*-states of C atom from below the core states. The second bands which lie at -5.45 eV and -2.402 eV are the energy bands of ZrC due to its *p* and *d*-state electrons of Zr atom and *p*-state electrons of C atom. Peaks occur at -2.39 eV and -2.76 at W point are p-state of C atom and *p* and *d*-state of Zr. From the plots of band structures we have found that all the energy bands show the behavior of electrons in metals. Hence, ZrC exhibit metallic nature.

V. Conclusions

For calculating PFEC we have used Green function in which the basis functions used were calculated by the projection operator method of group theory [1]. In this case, it is found that the behavior of PFEC as a function of applied field and initial state energy also shows similar trends as in the case of other metals like W.The variation of PFEC against the applied electric field decreases exponentially with the decrease in the applied field for both the cases as shown in Fig. 2 and Fig. 3. This is due to an exponential term is involved in the formula for transition probability *D(W)* which is given in Eq. (7).The origin of peak in initial state energy (E_i) of electrons at 2.396 eVin the valence bands below the Fermi level as shown in Fig. 2 is confirmed by the DOS plots of ZrC. For example, the total DOS plots gives maxima at 2.402 eV (Fig. 4) and from the partial DOS (Fig 5) we get peak at the occurrence of peak at 2.402 eV. This means that the origin of peaks at 2.396 eV below the Fermi level as shown in Fig.2 is due to contribution by mostly the *p* and *d*-states of Zr.

Acknowledgements

LND is grateful to Mizoram University UGC fellowship, GD, LP and RKT is grateful to UGC for sanctioning a research project. GD also acknowledges also the help rendered by Mr. B.S. Thapa, Principal, Govt. Kolasib Colleges, Kolasib, Mizoram for carrying out the research work.

References

[1]. R.K.Thapa and GunakarDas,*Modern Physics Letters B, 21(22)* 1501-1507(2007).
[2]. A. Bagchi and N. Kar, *Phys. Rev.B18* (1978) 5240-5247.
[3]. W. Kohn & L.J. Sham, *Phys. Rev.A140* (1965) 1133-1138.
[4]. P. Blaha, K. Schwarz, G. K. H. Madsen, D. Kvasnicka and J. Luitz, *Vienna Universitat of Technology, Vienna*(2001).
[5]. M.J.G. Lee, *Phys. Rev.30* (1973) 1193.
[6]. C. Schwartz and M.W. Cole, *Surf. Sci.95* (1975) 1243.
[7]. Y. Gao, R. Reifenberger, *Phys. Rev.B35* (1987) 4284.
[8]. C. Schwartz and W.L. Schaich. *Phys. Rev.B24* (1981) 1583.
[9]. J.T. Lee and W.I. Schaich, *Phys. Rev.B38* (1988) 3747.
[10]. T. Radon and S. Jaskolka, *Solid State Phenomena121* (1990) 63.
[11]. T. Radon, *Prog. Surf. Sci.59* (1998) 331, *67* (2001) 339.
[12]. C. Caroli, D. Lederer-Rozenblatt, B. Rowlet and D. Saht-James,*Phys. Rev.10* (1973) 163.
[13]. E. Taranko, *Acta Phys. Pol.A49* (1976) 721,*J. Phys.38* (1977) 163.
[14]. A. Bagchi, *Phys. Rev.B10* (1974) 542.
[15]. C. Schwartz and M.W. Cole, *Surf. Sci.115*(1982) 290-300.
[16]. R.K. Thapa and G. Das, *Intl. Jour. Mod. Phys.B19* (2005) 3141-3149.